

Efficient and robust Sensor Placement in Complex Environments

Lukas Taus¹ and Yen-Hsi Richard Tsai²

Abstract—We address the problem of efficient and unobstructed surveillance or communication in complex environments. On one hand, one wishes to use a minimal number of sensors to cover the environment. On the other hand, it is often important to consider solutions that are robust against sensor failure or adversarial attacks. This paper addresses these challenges of designing minimal sensor sets that achieve multi-coverage constraints — every point in the environment is covered by a prescribed number of sensors. We propose a greedy algorithm to achieve the objective. Further, we explore deep learning techniques to accelerate the evaluation of the objective function formulated in the greedy algorithm. The training of the neural network reveals that the geometric properties of the data significantly impact the network’s performance, particularly at the end stage. By taking into account these properties, we discuss the differences in using greedy and ϵ -greedy algorithms to generate data and their impact on the robustness of the network.

I. INTRODUCTION

In this paper, we focus on the problem of sensor placement in environments with obstacles blocking the sensors’ lines of sight. The sensors that we have in mind include conventional cameras (passive observations) and LIDARs or other active sensors that emit and receive high-frequency signals. Depending on the sensor type, the problem is that of surveillance or communication. The goal is to place a minimal number of sensors so that multiple sensors can observe each point in the environment. The motivation for such a problem is to improve the robustness of the sensor network against sensor failure and adversarial attacks. Naturally, the need

for solving such type of constrained optimization problems can be found in many practical problems. The placement of 5G towers, for example, could benefit from optimal solutions to the multi-coverage constraints to improve the robustness of communication against signal loss due to blockage.

Due to the constraint of requiring multiple sensors to observe the free space in the environment, finding optimal configurations of a minimal set of sensors requires a daunting computational complexity. We propose a greedy approach, accelerated by deep learning, to efficiently generate a sequence of sensor locations that achieve multi-coverage for most free space. We also present numerical experiments illustrating results for real-life urban environments.

A. RELATED WORKS

Finding optimal sensor locations for a known environment is related to the gallery problem in computational geometry. For polygonal environments with n vertices and h holes it was shown in [24] [25] that $\lfloor (n+h)/3 \rfloor$ sensors are sufficient. However, determining the optimal sensor locations for an environment was shown to be NP-complete in [14] [15] [16]. For more general environments, an alternating minimization scheme [26] and a system of differential equations [27] were proposed. Both methods assume that the number of sensors is fixed. For general 2D environments, Landa et al. [2] [5] [6] propose to place sensors along frontiers, the boundary between the observed and occluded space. However, it is not necessarily optimal to choose sensor locations along the frontiers [28]. For general 3D environments, a level set representation is used to calculate visible regions [3] [4]. For environments that are given by a graph

^{1,2}Oden Institute for Computational Engineering and Sciences, The University of Texas at Austin

¹l.taus@utexas.edu

²ytsai@math.utexas.edu

of a function, a method to construct volumetric visibility information was discussed in [11]. A common measure of information gain is the volume of the unexplored region within sensor range [17] [18] [19] [20]. However, other measures like the surface area of frontiers weighted by the view angle [7] [8] have also been used. This information can be used in greedy algorithms where a sequence of sensor locations is generated through maximization of the used measure [1]. Using the gained volume of observed space as a gain function and approximating it using deep learning techniques was considered in [13]. In addition to achieving visibility, it is also indispensable in practice to account for depth-sensor errors by considering uncertainty quantification. Popović et al. proposed a method to accurately estimate the occlusion map from faulty or incomplete depth measurements [12].

II. MULTI-COVERAGE FORMULATION

We consider the task of generating a sequence of sensor locations to achieve visibility in a given environment, using as few sensors as possible. At the same time, we propose that multiple sensors can observe the same region of the environment. This multi-coverage constraint would increase the robustness of surveillance against sensor failure or possible imperfection in the given information about the environment. Even when one sensor fails, it is still possible to observe the full environment. When the sensors are depth sensors, it also provides improved confidence in the depth measurement since we can access multiple measurements to the same surface from different angles. This is especially important when the depth sensors are unreliable due to the surface properties of the environment, e.g. reflective surfaces.

A. The order of visibility

Consider an environment $\Omega \subset \mathbb{R}^d$, $d=2,3$. The environment consists of two disjoint sets: an open set Ω_{free} which describes the free space and a closed set $\Omega_{\text{obs}} := \Omega \setminus \Omega_{\text{free}}$ which describes the space that is covered by some obstacle.

For line-of-sight-coverage, define the relation between any pair of points in Ω :

$$x \overset{\text{vis}}{\sim} y \iff \forall \lambda \in [0, 1] : \lambda x + (1 - \lambda)y \in \Omega_{\text{free}}. \quad (1)$$

We define the "order of visibility" map by

Definition 2.1: (Order of visibility map) Given an environment Ω and sensors $x_1, x_2, \dots, x_n \in \Omega_{\text{free}}$. The order of visibility at a point $y \in \Omega_{\text{free}}$ is defined by

$$\mathcal{O}_{\text{vis}}(y; x_1, x_2, \dots, x_n) = \sum_{i=1}^n \Phi(y; x_i),$$

where $\Phi(y, x_i)$ is the indicator function of $y \overset{\text{vis}}{\sim} x_i$. Note that two sensors x_i and x_j might be in the same location i.e. $x_i = x_j$. In the following we will also use the notation $\mathcal{O}_{\text{vis}}(y; P_n)$ for a set of sensors $P_n = \{x_1, \dots, x_n\}$ for the above. We illustrate the concept of visibility order in Figure 1.

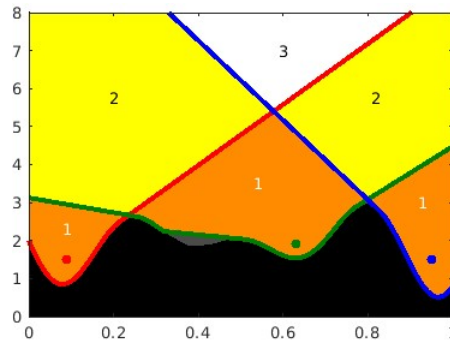


Fig. 1: The order of visibility of three sensors (red, blue, and green). Here Ω_{free} is the area above the black curve on the bottom.

Thus we can describe our objective as follows:

Find the minimal number of sensors
 $P_n = \{x_1, \dots, x_n\}$ such that
 $\text{Vol}(\{y \in \Omega \mid \mathcal{O}_{\text{vis}}(y; P_n) \geq k\}) = \delta \text{Vol}(\Omega_{\text{free}}). \quad (2)$

Solving this problem yields a sequence of sensor locations x_1, \dots, x_n such that a threshold $\delta \in (0, 1)$ of the free space of the environment Ω_{free} is observed by at least k sensors.

Unfortunately, this problem is computationally very complex. Even when the environment is a polygon with n vertices and h holes, calculating optimal locations is an NP-complete problem [14] [15] [16]. Other methods work for more general environments, but the amount of sensors needed is assumed to be known [26] [27].

For simplicity, we consider obstacle maps that are given by a graph of a function f via

$$(x_1, \dots, x_n) \in \Omega_{\text{free}} \iff f(x_1, \dots, x_{n-1}) < x_n.$$

Consequently, one can prove that If the environment is described by a function f . Then for any $y \in \Omega_{\text{free}}$ there exists a function g_y such that

$$y \stackrel{\text{vis}}{\sim} x = (x_1, \dots, x_n) \iff g_y(x_1, \dots, x_{n-1}) < x_n.$$

This means that the visibility from the locations x_1, \dots, x_n can be described by the graph of the function g_y .

While this assumption reduces the dimension of the underlying problem, it still allows complicated environment geometries. Nevertheless, we remark that the proposed greedy approach and the accompanying Deep Learning strategy to be described below do not really depend on this assumption on the environment.

III. GREEDY ALGORITHMS

To solve this problem in a feasible time greedy algorithms are used to calculate approximate solutions. They involve generating a sequence of sensors one by one where the next point is chosen by maximizing some objective function. We call the value of such an objective function at a point x , the gain at x . For our problem, a natural choice of the objective function would be the gain of observed area up to order k . Define for any set of sensors the function

$$\Psi_k(P) = \int_{\Omega_{\text{free}}} \min(\mathcal{O}_{\text{vis}}(y; P), k) dy.$$

Then the gain function for some given set of sensors $P_m = \{x_1, \dots, x_m\}$ is defined as

$$\mathcal{G}_{\text{naive}}(x; P_m) := \Psi_k(P_m \cup \{x\}) - \Psi_k(P_m). \quad (3)$$

However, as the following Proposition shows, this naïve choice of objective function will lead to trivial and non-optimal solutions.

Proposition 3.1: Suppose $P_m = \{x_1, \dots, x_m\}$ are generated by

$$x_{m+1} \in \arg \max_{x \in \Omega_{\text{free}}} \mathcal{G}_{\text{naive}}(x; P_m)$$

and

$$\forall y \in \{z \in \Omega_{\text{free}} | z \stackrel{\text{vis}}{\sim} x_m\}: \mathcal{O}(y; P_{m-1}) < k - 1$$

where k is the target order of visibility. Then

$$x_{m+1} \in \arg \max_{x \in \Omega_{\text{free}}} \mathcal{G}_{\text{naive}}(x; P_{m-1}).$$

This shows that when the target order k has been reached nowhere, then the next sensor will be chosen from the same pool as the previous one. Since this condition is always satisfied in the beginning if $k \geq 2$ and it is rare that two sensors have equal gain, the sensor will be chosen repeatedly. This will yield the trivial solution which places k sensors in the same location. In most applications however, this solution is not desirable. It provides little robustness towards adversarial attacks and does not improve confidence in the depth sensors since it does not yield additional measurements from different angles.

We therefore use the following objective function which enforces distance between sensors.

$$\mathcal{G}_k(x; P_n) := \min_{i=1, \dots, n} \|x - x_i\|_p \mathcal{G}_k^{\text{naive}}(x; P_n), \quad (4)$$

where $\|\cdot\|_p$ is the ℓ_p norm of a vector in \mathbb{R}^d and $P_n = \{x_1, \dots, x_n\}$. In this paper, $d = 2$ and $p = 2$.

Algorithm 1 ϵ -greedy algorithm

```

P = list()
while  $\int_{\Omega_{\text{free}}} \min(\mathcal{O}(y; P), k) dy < \delta k \lambda(\Omega_{\text{free}})$  do
  calculate  $\mathcal{G}_k(x, P)$  for every  $x \in \Omega_{\text{free}}$ 
  calculate  $M = \max_{z \in \Omega_{\text{free}}} \mathcal{G}_k(z, P)$ 
  choose  $x^*$  randomly from the set
   $\{y \in \Omega_{\text{free}} | \mathcal{G}_k(y, P) \geq (1 - \epsilon)M\}$ 
  P.append( $x^*$ )
end while

```

We present Algorithm 1, which describes an ϵ -greedy method to generate a sequence of sensors stored in P . If $\epsilon = 0$ we just call it the greedy algorithm. k describes the target order of

visibility and δ describes the termination threshold percentage of Ω_{free} (or Ω_{vis}). However this is still costly to evaluate $\mathcal{G}_k(x, P)$ for every $x \in \Omega_{\text{free}}$.

For $k = 1$, It is possible to derive a submodularity theory [29] to derive bounds that compare the relative performance of the greedy algorithm compared to the optimal solution; see [1]. However when using the modified objective function \mathcal{G}_k as an analog to the discrete derivative the submodular property is lost.

A. Remark on computational complexity.

Using the sweeping algorithm for graph environments from [11] has a computational complexity of $\mathcal{O}(M^2)$ for the evaluation of \mathcal{G}_k . Thus using the ϵ -greedy algorithm, placing K sensors on an $M \times M$ grid in $\Omega_{\text{free}} \subset \mathbb{R}^2$ has complexity of $\mathcal{O}(KM^2)$. We can observe that most of the complexity stems from the evaluation of the gain function. While this is much faster than a brute-force search of sensor sets, the evaluation of the gain function can still be costly for large environments.

IV. GREEDY ALGORITHMS AIDED BY DEEP LEARNING

Above we explained that the computational cost associated with each greedy step for adding a new sensor remains notably high. To address this challenge, we present a deep learning approach in this section, building upon the strategy introduced in [13], with the aim of significantly improving computational speed.

Our method involves a neural network, denoted as $G_{k,\theta}[X_0; D_N]$, trained using the data set D_N . This neural network, trained with a suitable data set D_N , approximates the gains $\mathcal{G}_k(x_{i,j})$ for $x_{i,j}$ on a grid over the environment, thereby enhancing computational efficiency. We will delve into the critical aspects of "generating" a performing training data set D_N , essential to the success of our approach.

A. Network architecture

We used the network architecture called TiraFL described in [10]. For the order $k = 1$ visibility case, it was shown in [13] that a UNet architecture is capable of approximating the gain function.

However in our experiments a UNet architecture of similar size performed poorly for higher orders of visibility $k > 1$.

B. Training data

As in the supervised learning setup, the data points in our study take the form of data pairs: (X, Y) . The input data X is composed of two parts, namely X_{obs} and X_{cumvis} .

X_{obs} represents the "obstacle/environment map". For the data generation we used Massachusetts building footprint maps from [9] (The labels specifically). From this data set, we used random crops and a flood fill algorithm to assign random heights (between 0 and 1) to each distinguishable building to extend it to a 3D obstacle map. For these maps, we do not allow placements of sensors on top of buildings.

X_{cumvis} is the "cumulative visibility map," which provides the coverage information of a given set of sensors, and requires simulating the greedy algorithms offline, starting from a random initialization of the first sensor. Since

$$y \stackrel{\text{vis}}{\sim} x = (x_1, \dots, x_n) \iff g_y(x_1, \dots, x_{n-1}) < x_n,$$

we see that

$$\mathcal{O}_{\text{vis}}(y; x^1, x^2, \dots, x^n) = \ell \iff$$

$$\ell\text{-min}\{g_{x^i}(y_1, \dots, y_{n-1}) : i = 1, \dots, N\} < y_n,$$

where $\ell\text{-min}$ returns the ℓ -th smallest element in the given set. For convenience, we define $C_\ell(y) = \ell\text{-min}\{g_{x^i}(y_1, \dots, y_{n-1}) : i = 1, \dots, N\}$. Using this representation we can derive a simple update rule for C_ℓ when adding a new sensor $x \in \Omega_{\text{free}}$:

$$C_\ell(y) \leftarrow \ell\text{-min}\{C_1(y), \dots, C_k(y), g_x(y_1, \dots, y_{n-1})\}.$$

The output data Y is the image of \mathcal{G}_k on a grid overlaying the environment described by X_{obs} . Further both the input and gain are normalized such that each element is in $[0, 1]$. Depending on the specific greedy algorithm used to generate X_{cumvis} (and consequently Y), we denote the corresponding datasets as $D_{N_1}^0$ for the pure greedy

approach and $D_{N_2}^\epsilon$ for the ϵ -greedy method.

TABLE I: Data sets used in our study.

	D_N^0	D_N^ϵ	D_N^+
N	6531	2511	6342 (3831+2511)
ϵ	0	0.05	0 and 0.05
Grid	128×128	128×128	128×128
Order	2	2	2

D_N^0 was generated using the greedy algorithm with $\epsilon = 0$. D_N^ϵ was generated using the ϵ greedy algorithm with $\epsilon = 0.05$. Notably, $D_N^+ = D_{N_1}^0 \cup D_{N_2}^\epsilon$ combines both types of data for comprehensive analysis and comparison. The merged data set only contains a subset of D_N^0 to keep the number of data points in D_N^+ and $D_{N_1}^0$ at a similar level. We will see, in Section V, that this combined dataset leads to performing neural networks.

V. EFFECT OF DATA GEOMETRY

In this section, we analyze the networks trained with D_N^0 and D_N^+ in an urban environment. Accurate results can be observed when looking at test data, however, this only checks the accuracy of one step. As the network is the approximation of the gain function, it needs to be applied multiple times where its input depends on the output of the previous iteration. Initially, the network's predictions are accurate, but its reliability diminishes as the simulation progresses. This decrease in accuracy typically occurs when the network encounters a scenario where two or more sensors, which are far apart, produce a similar gain. Due to approximation error, the network may choose a sub-optimal option in these cases, resulting in decreased accuracy for future placements.

Note that the gain function from Equation (4) cannot be evaluated when no sensors have been placed. Hence, we fix the first sensor at $(0, 0)$. Then we generate the subsequent sensors using the methods discussed above. As a reference, we will use the greedy algorithm where the function \mathcal{G}_k is calculated and the maximal value is chosen.

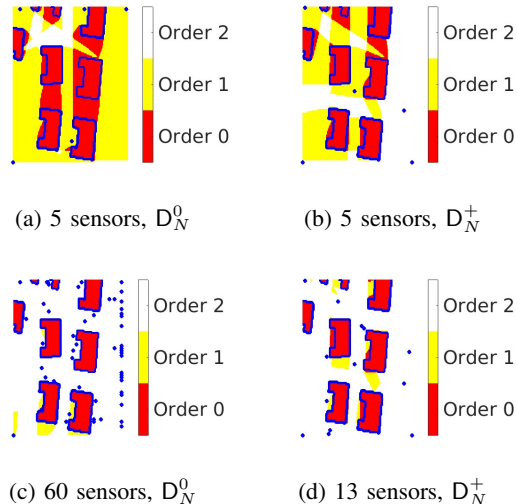


Fig. 2: Comparison of order of visibility function when using the neural network trained with D_N^0 and D_N^+ . The first row shows the result after placing 5 sensors. The second row shows the result after the threshold volume was reached.

In Figure 2, we see that both neural networks show promising results for the first 5 sensors. However, as shown in the bottom row for later iteration the neural network trained with D_N^0 predicts close points repeatedly. This can be observed by the accumulation of blue dots (sensors) on the right side. The network trained with D_N^+ however performs well throughout the whole algorithm and achieves target volume after placing 13 sensors.

To gain further insight, we delve into the data geometry of both data sets, with a particular focus on later stages in the simulation. We hope to shed light on the mechanisms that underlie the improved performance of the extended data set. To conduct this analysis, we initially extracted data points from the training data set that corresponded to either the final 10 sensors placed or the second half of the data when fewer than 20 points were required to reach the visibility threshold. This data set is then centered around its mean and PCA is applied to extract the principle directions and the corresponding singular values. We then compare the singular values to get insight into the data geometries in Figure 3.

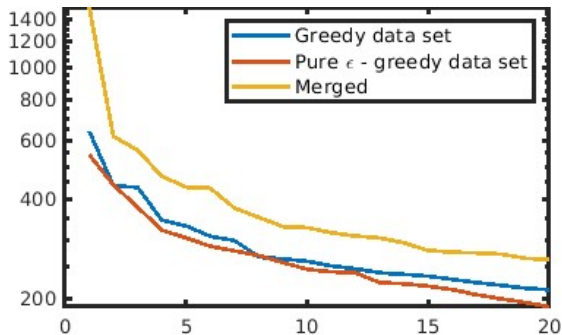


Fig. 3: Comparison of the first 20 singular values of data sets in final stages of placement. The x-axis depicts the number of the singular values ordered by their magnitude and the y-axis depicts the value of the singular values.

The singular values describe the variances of the data set in the associated principal (singular) direction. While the dimensionality of the Greedy and ϵ -greedy data sets are similar, the merged data set is higher dimensional. This may explain the bad predictions in the later stages of the simulation for the greedy data set.

VI. DEMONSTRATION

With the trained network, the computation for each greedy step is 105 times faster when using 64 cores on an AMD EPYC 7763 CPU for the greedy algorithm and a NVIDIA A100 GPU for the network approximation. In Figure 4, we compare the distributions of the number of sensors needed to reach a prescribed threshold.

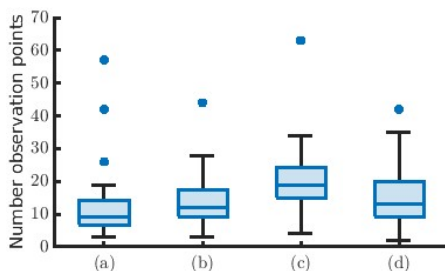


Fig. 4: Distribution of the number of sensors needed for 54 urban obstacle maps. Shows the results for (a) \mathcal{G}_k with $\epsilon = 0$. (b) neural network trained with D_N^+ . (c) Random sensor placement. (d) neural network trained with $D_{N_1}^0$

The neural network trained with D_N^+ produces results comparable to using calculation of the function \mathcal{G}_k . Thus we can use the neural network to efficiently approximate the gain function which allows for a fast application of the greedy algorithm for 3D urban maps.

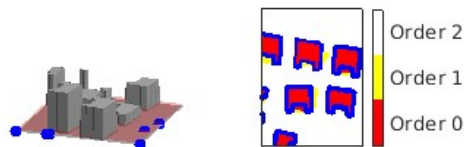


Fig. 5: Horizontal slice

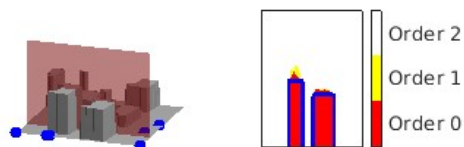


Fig. 6: Vertical slice

We present the final results of the greedy algorithm using the neural network in Figures 5-6. The red plane on the left represents slices of the order of the visibility map shown on the right.

VII. SUMMARY

We propose a greedy algorithm for placing a minimal set of sensors that satisfies a multi-coverage requirement. We show that the framework can be well approximated using deep learning techniques for a broad class of obstacles, which significantly improves computation time. The geometric properties of the data used for training play an important role in the accuracy and variability in generating the training data is crucial for the success of the algorithm. We envision that the insight into data geometry has large implications for neural network approximation tasks.

VIII. ACKNOWLEDGEMENT

Taus is supported by Army Research Office, under Cooperative Agreement Number W911NF-19-2-0333. Tsai is partially supported by Army Research Office, under Cooperative Agreement Number W911NF-19-2-0333 and National Science Foundation Grant DMS-2110895.

REFERENCES

- [1] Ly, L. & Tsai, Y. Greedy Algorithms for Sparse Sensor Placement via Deep Learning. *ArXiv Preprint arXiv:1809.06025*. (2018)
- [2] Landa, Y., Tsai, R. & Cheng, L. Visibility of point clouds and mapping of unknown environments. *Advanced Concepts For Intelligent Vision Systems: 8th International Conference, ACIVS 2006, Antwerp, Belgium, September 18-21, 2006. Proceedings 8*. pp. 1014-1025 (2006)
- [3] Cheng, L. & Tsai, Y. Visibility optimization using variational approaches. (2005)
- [4] Tsai, Y., Cheng, L., Osher, S., Burchard, P. & Sapiro, G. Visibility and its dynamics in a PDE based implicit framework. *Journal Of Computational Physics*. **199**, 260-290 (2004)
- [5] Landa, Y. & Tsai, R. Visibility of point clouds and exploratory path planning in unknown environments. *Communications In Mathematical Sciences*. **6**, 881-913 (2008)
- [6] Landa, Y., Galkowski, D., Huang, Y., Joshi, A., Lee, C., Leung, K., Malla, G., Treanor, J., Voroninski, V., Bertozzi, A. & Others Robotic path planning and visibility with limited sensor data. *American Control Conference, 2007. ACC'07*. pp. 5425-5430 (2007)
- [7] Valente, L., Tsai, Y. & Soatto, S. Information gathering control via exploratory path planning. *2012 46th Annual Conference On Information Sciences And Systems (CISS)*. pp. 1-6 (2012)
- [8] Valente, L., Tsai, Y. & Soatto, S. Information-seeking control under visibility-based uncertainty. *Journal Of Mathematical Imaging And Vision*. **48**, 339-358 (2014)
- [9] Mnih, V. Machine Learning for Aerial Image Labeling. (University of Toronto, 2013)
- [10] Jégou, S., Drozdal, M., Vazquez, D., Romero, A. & Bengio, Y. The One Hundred Layers Tiramisu: Fully Convolutional DenseNets for Semantic Segmentation. (2017)
- [11] Kao, C. & Tsai, R. Properties of a Level Set Algorithm for the Visibility Problems. *J. Sci. Comput.* **35** pp. 170-191 (2008,6)
- [12] Popović, M., Thomas, F., Papatheodorou, S., Funk, N., Vidal-Calleja, T. & Leutenegger, S. Volumetric Occupancy Mapping With Probabilistic Depth Completion for Robotic Navigation. *IEEE Robotics And Automation Letters*. **6**, 5072-5079 (2021)
- [13] Ly, L. & Tsai, Y. Autonomous Exploration, Reconstruction, and Surveillance of 3D Environments Aided by Deep Learning. *2019 International Conference On Robotics And Automation (ICRA)*. pp. 5467-5473 (2019)
- [14] Urrutia, J. Chapter 22 - Art Gallery and Illumination Problems. *Handbook Of Computational Geometry*. pp. 973-1027 (2000)
- [15] O'Rourke, J. & Supowit, K. Some NP-hard polygon decomposition problems. *IEEE Transactions On Information Theory*. **29**, 181-190 (1983)
- [16] Lee, D. & Lin, A. Computational complexity of art gallery problems. *IEEE Transactions On Information Theory*. **32**, 276-282 (1986)
- [17] González-Baños, H. & Latombe, J. Navigation Strategies for Exploring Indoor Environments. *I. J. Robotic Res.* **21** pp. 829-848 (2002,10)
- [18] Bircher, A., Kamel, M., Alexis, K., Oleynikova, H. & Siegwart, R. Receding Horizon "Next-Best-View" Planner for 3D Exploration. (2016,5)
- [19] Bircher, A., Kamel, M., Alexis, K., Oleynikova, H. & Siegwart, R. Receding horizon path planning for 3D exploration and surface inspection. *Autonomous Robots*. **42** (2018,2)
- [20] Heng, L., Gotovos, A., Krause, A. & Pollefeys, M. Efficient visual exploration and coverage with a micro aerial vehicle in unknown environments. *Proceedings - IEEE International Conference On Robotics And Automation*. **2015** pp. 1071-1078 (2015,6)
- [21] Goodrich, B., Kuefler, A. & Richards, W. Depth by Poking: Learning to Estimate Depth from Self-Supervised Grasping. *2020 IEEE International Conference On Robotics And Automation (ICRA)*. pp. 10466-10472 (2020)
- [22] Chen, M., Herbert, S., Hu, H., Pu, Y., Fisac, J., Bansal, S., Han, S. & Tomlin, C. FaSTrack: A Modular Framework for Real-Time Motion Planning and Guaranteed Safe Tracking. *IEEE Transactions On Automatic Control*. **66**, 5861-5876 (2021,12), <https://doi.org/10.1109>
- [23] Ly, L. & Tsai, Y. Autonomous Exploration, Reconstruction, and Surveillance of 3D Environments Aided by Deep Learning. *CoRR*. **abs/1809.06025** (2018), <http://arxiv.org/abs/1809.06025>
- [24] Bjorling-Sachs, I. and Souvaine, D. An efficient algorithm for guard placement in polygons with holes. *Discrete & Computational Geometry*. **13** pp. 77-109 (1995), <https://api.semanticscholar.org/CorpusID:37188717>
- [25] Hoffmann, F., Kaufmann, M. & Kriegel, K. The art gallery theorem for polygons with holes. [1991] *Proceedings 32nd Annual Symposium Of Foundations Of Computer Science*. pp. 39-48 (1991)
- [26] Goroshin, R., Huynh, Q. & Zhou, H. Approximate solutions to several visibility optimization problems. *Communications In Mathematical Sciences*. **9** (2011,6)
- [27] Kim, S., Kang, S. & Zhou, H. Optimal Sensor Positioning (OSP); A Probability Perspective Study. (2016)
- [28] Ghosh, S., Burdick, J., Bhattacharya, A. and Sarkar, S. Online Algorithms with Discrete Visibility - Exploring Unknown Polygonal Environments. *IEEE Robotics & Automation Magazine*. **15**, 67-76 (2008)
- [29] Krause, A. & Golovin, D. Submodular Function Maximization. *Tractability*. **3** pp. 71-104 (2011,1)
- [30] Taus, L. Code Base for k-Visibility. (2023), <https://github.com/tsai-lab-ut/k-Visibility>
- [31] Uwaechia, A. & Mahyuddin, N. A Comprehensive Survey on Millimeter Wave Communications for Fifth-Generation Wireless Networks: Feasibility and Challenges. *IEEE Access*. **8** pp. 62367-62414 (2020)